P_i^s vapor pressure of pure component i
q pure-component area parameter
R universal gas constant
r pure-component volume parameter
T absolute temperature
V true molar volume of alcohol mixture
V° true molar volume of pure alcohol solution
v_i^L molar volume of pure liquid i
x liquid mole fraction
y vapor mole fraction
Z coordination number equal to 10

Greek Letters

γ_I liquid-phase coefficient
θ area fraction
σ_P, σ_T standard deviations in pressure and temperature
σ_x, σ_y standard deviations in liquid and vapor mole fractions
τ_{IJ} $\exp(-a_{IJ}/T)$
ϕ_i fugacity coefficient of component i
ϕ_i^s fugacity coefficient of pure component i at its saturation pressure
Φ_A, Φ_B, Φ_C segment fractions of components A, B, and C
Φ_{A_1} segment fraction of alcohol monomer
$\Phi^\circ_{A_1}$ segment fraction of alcohol monomer in pure alcohol solution
Φ_{OB} segment fraction of chloroform monomer in mixture
Φ_{OC} segment fraction of benzene monomer in mixture

Registry No. 2-Propanol, 67-63-0; chloroform, 67-66-3; benzene, 71-43-2.

Literature Cited

(1) Nagata, I.; Ohta, T.; Uchiyama, Y. *J. Chem. Eng. Data* **1973**, *18*, 54-9.
(2) Nagata, I.; Hayashida, H. *J. Chem. Eng. Jpn.* **1970**, *3*, 161-6.
(3) Ohta, T.; Koyabu, J.; Nagata, I. *Fluid Phase Equilib.* **1981**, *7*, 65-73.
(4) Spencer, C. F.; Danner, R. P. *J. Chem. Eng. Data* **1972**, *17*, 236-41.
(5) Hayden, J. G.; O'Connell, J. P. *Ind. Eng. Chem. Process Des. Dev.* **1975**, *14*, 209-16.
(6) Vera, J. H.; Sayegh, C. G.; Ratcliff, G. A. *Fluid Phase Equilib.* **1977**, *1*, 113-35.
(7) Nagata, I.; Kawamura, Y. *Chem. Eng. Sci.* **1979**, *34*, 601-11.
(8) Brandani, V. *Fluid Phase Equilib.* **1983**, *12*, 87-104.
(9) Prausnitz, J. M.; Anderson, T. F.; Grens, E. A.; Eckert, C. A.; Hsieh, R.; O'Connell, J. P. "Computer Calculations for Multicomponent Vapor-Liquid and Liquid-Liquid Equilibria"; Prentice-Hall: Englewood Cliffs, NJ, 1980; Chapters 3 and 4, Appendix D.

Received for review April 2, 1984. Accepted June 22, 1984.

Liquid–Liquid–Vapor Immiscibility Limits in Carbon Dioxide + *n*-Paraffin Mixtures

David J. Fall, Jaimie L. Fall, and Kraemer D. Luks*

Department of Chemical Engineering, The University of Tulsa, Tulsa, Oklahoma 74104

Liquid–liquid–vapor equilibria for the binary systems CO_2 + *n*-nonadecane and CO_2 + *n*-heneicosane were studied. Liquid–liquid–vapor data on the binary mixture CO + *n*-eicosane were also taken and compared with an earlier study in the literature. For the homologous series of *n*-paraffins it appears that the extent of the liquid–liquid–vapor immiscibility decreases from a maximum at carbon number 14 to carbon number 21. The liquid–liquid–vapor locus has a length of about 3.0 K for CO_2 + *n*-heneicosane and is nonexistent for carbon number 22 and higher. Also studied were solid–liquid–vapor equilibria for CO_2 + *n*-nonadecane and CO_2 + *n*-heneicosane and liquid–vapor isotherms for CO_2 + *n*-nonadecane at 40 and 60 °C and CO_2 + *n*-heneicosane at 45 and 65 °C.

Introduction

In this paper we report on the occurrence of liquid–liquid–vapor (LLV) equilibria in the homologous series of binary CO_2 + *n*-paraffin mixtures. Specifically, phase equilibria data are presented that identify the limit of LLV immiscibility in this series of mixtures. In addition to the LLV data on the binary systems, liquid–vapor (LV) and solid–liquid–vapor (SLV) data are also presented. These data are helpful in understanding the occurrence of LLV behavior in complex mixtures such as CO_2 + oil systems that are encountered in CO_2-enhanced recovery processes. A quantitative description of these binary systems is useful in supporting the development of equations-of-state purporting to be applicable to these multicomponent systems.

LLV immiscibility has been observed in CO_2 + *n*-paraffin binary systems ranging from *n*-heptane (*1*) to *n*-eicosane (*2*). Schneider et al. (*3–5*) performed early studies showing LLV immiscibility in the CO_2 + *n*-paraffin binary systems with *n*-octane, *n*-undecane, *n*-tridecane, and *n*-hexadecane. Hottovy et al. (*6*) detailed the LLV behavior of the binary systems containing *n*-dodecane to *n*-pentadecane, while Kulkarni et al. (*7*) studied the CO_2 + *n*-decane system along its multiphase loci, including LLV. It was learned from the Hottovy and Schneider studies that there is a transition in the nature of the LLV loci between the *n*-tridecane and *n*-tetradecane species and that the greatest extent of LLV locus occurs with *n*-tetradecane, which had an LLV locus extending from an upper critical end point, or K point (L–L=V), at 311.15 K to a quadruple point, or Q point (SLLV), at 269.10 K.

Obviously, the occurrence of LLV behavior in the CO_2 + *n*-paraffin binary system homologous series must eventually disappear as the molecular nature of the CO_2 and the *n*-paraffin become too diverse to support the existence of an LLV locus. In particular, if the triple point of the *n*-paraffin occurs at a temperature too far above the critical point of CO_2, then the binary SLV locus that evolves from the triple point of the *n*-paraffin will be located too high in temperature to form a lower terminus (SLLV) to an LLV locus.

In this paper, data will be presented for the binary systems CO_2 + *n*-nonadecane and CO_2 + *n*-heneicosane along their LLV loci and compared with earlier studies on the binary systems CO_2 + *n*-eicosane and CO_2 + *n*-docosane. Also presented will be the data along the SLV loci of these binary systems and along two nearby LV isotherms for each of the systems. A discussion will follow focusing on the relative location

0021-9568/85/1730-0082$01.50/0

in thermodynamic phase space of the LLV and SLV three-phase loci for the homologous series of CO_2 + *n*-paraffin binary systems, which determines the LLV immiscibility limit in the series of systems.

Experimental Apparatus and Procedures

A detailed description of the experimental apparatus is given in an earlier paper by us (*8*). The procedures for performing SLV and LV studies are presented in the same reference. Briefly summarizing those procedures, for an LV study, a known amount of a *n*-paraffin is placed in a 7.5-mL visual (glass) equilibrium cell. During an experimental run, measured amounts of CO_2 gas are added to the thermostated visual cel from a high-pressure bomb by means of a manual (Ruska) pump. By a careful mass balance, the moles of CO_2 in the liquid phase can be determined (the vapor phase is assumed to be pure CO, due to the low volatility of the *n*-paraffins in this study at the temperatures of interest). An SLV study is conducted in a similar manner but with a trace amount of solid phase (*n*-paraffin) being present in equilibrium with the liquid and vapor phases.

In doing an experimental LLV run, one takes conjugate measurements at a given temperature, in which one measurement has a large amount of L_1 relative to L_2 present ("L_1-dominant") and the second measurement has $L_2 \gg L_1$ ("L_2-dominant"). Lever principles (mass balances) can be applied so that compositions and molar volumes of L_1 and L_2 can be computed. The equations that result from the lever principle analysis are presented in the Appendix. The termination points of the LLV loci are determined individually by straightforward visual observation.

Temperature is measured with a Pt-resistance thermometer to an estimated accuracy of ±0.02 K while pressure is measured to ±0.07 bar (1 psia) with pressure transducers which are frequently calibrated against an accurate dead-weight gauge. Phase volumes in the calibrated visual cell are determined by a cathetometer to an accuracy of ± 0.005 mL.

Materials

The *n*-nonadecane and *n*-heneicosane were purchased from Alfa Products with a stated purity of 99%. Their melting points were determined to be 31.67 ± 0.05 and 40.16 ± 0.05 °C, respectively. The *n*-eicosane was purchased from Aldrich Chemical Co., Inc., with a stated purity of 99%. Its melting point was determined to be 36.75 ± 0.05 °C. All the *n*-paraffins were used without further purification.

The CO_2 was obtained from Air Products and Chemicals, Inc. as "Coleman Grade" with a purity rating of 99.99%. It was transferred to an initially evacuated storage bomb as a liquid at about 0 °C. In this two-phase condition, the vapor phase was vented and discarded to remove light gas impurities. Samples of the remaining CO_2 were liquefied in the visual cell at 25.00 °C and the pressure difference in the bubble and dew points was observed. This procedure generally produced a CO_2 supply with a pressure difference ranging from 0.5 to 2.0 psi. The vapor pressure at 25.00 °C and the critical temperature and pressure agreed with the literature values (*9*) to within ±0.07 bar (1 psia) and ±0.06 K, which is within the experimental accuracy of the visual cell technique in question for determining the location of a pure-component critical point.

Results

Table I presents raw data for the liquid-phase composition and molar volume of the binary LV system CO_2 + *n*-nonadecane at 40 and 60 °C. Table II presents raw data for the SLV locus of the same binary system. Figures 1 and 2 show the composition and molar volume data of Tables I and II collectively.

Table I. Pressure, Liquid-Phase Composition, and Molar Volume Raw Data for Liquid-Vapor Isotherms of Carbon Dioxide + *n*-Nonadecane

press., bar	$[CO_2]$, mole fraction	molar vol, mL/(g-mol)
Temperature = 40 °C (313.15 K)		
11.18	0.1335	306.0
12.83	0.1540	300.4
20.79	0.2378	275.1
23.92	0.2728	264.8
30.65	0.3328	247.0
36.40	0.3841	231.2
41.53	0.4253	219.4
49.84	0.4895	200.3
61.71	0.5695	175.4
62.29	0.5742	174.8
70.95	0.6290	158.4
71.81	0.6342	156.4
79.05	0.6770	144.6
Temperature = 60 °C (333.15 K)		
9.36	0.0899	325.0
11.03	0.1077	317.9
14.53	0.1512	304.0
18.97	0.1906	294.2
21.87	0.2153	285.5
25.37	0.2509	273.9
28.54	0.2749	268.1
31.85	0.3004	259.3
35.88	0.3348	248.4
38.16	0.3483	245.1
41.99	0.3748	236.1
45.64	0.4039	227.2
49.42	0.4248	221.9
52.37	0.4435	215.2
55.86	0.4691	207.2
59.20	0.4848	203.5
62.98	0.5087	195.3
66.56	0.5293	188.8
69.39	0.5409	186.2
73.02	0.5621	178.7
75.89	0.5768	174.5
79.58	0.5912	170.8

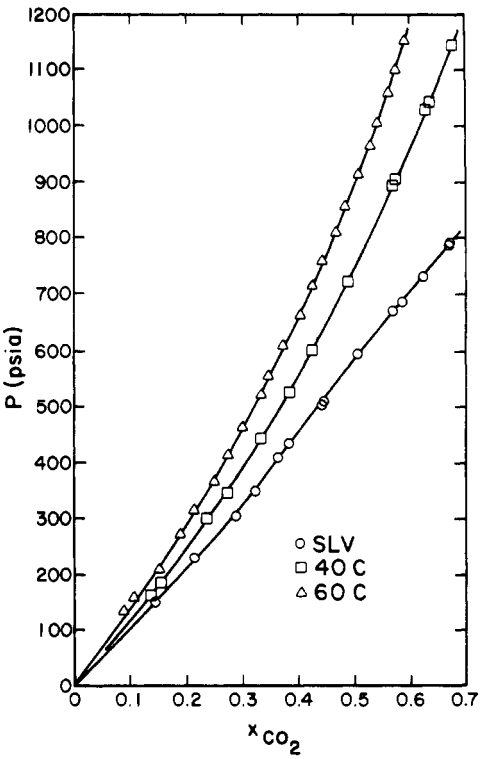

Figure 1. Pressure vs. liquid-phase mole fraction of CO_2 for the binary system CO_2 + *n*-nonadecane (14.5 psia = 1 bar).

Table II. Temperature, Pressure, Liquid-Phase Composition, and Molar Volume Raw Data for the Solid-Liquid-Vapor Locus of Carbon Dioxide + *n*-Nonadecane

temp, K	press., bar	$[CO_2]$, mole fraction	molar vol, mL/(g-mol)
302.86	10.40	0.1439	301.0
301.56	16.06	0.2134	280.9
300.45	21.13	0.2892	255.1
299.94	24.06	0.3215	246.8
298.86	28.25	0.3614	235.5
298.77	29.90	0.3822	228.4
297.42	34.53	0.4420	208.6
297.32	35.10	0.4459	208.6
295.99	40.94	0.5063	192.2
294.78	46.24	0.5691	173.9
294.69	47.40	0.5867	165.2
294.01	50.36	0.6224	156.0
293.23	54.42	0.6702	143.7
293.31	54.61	0.6710	143.3
292.88	57.18[a]		

[a] Q-point location, L_1 phase dominant.

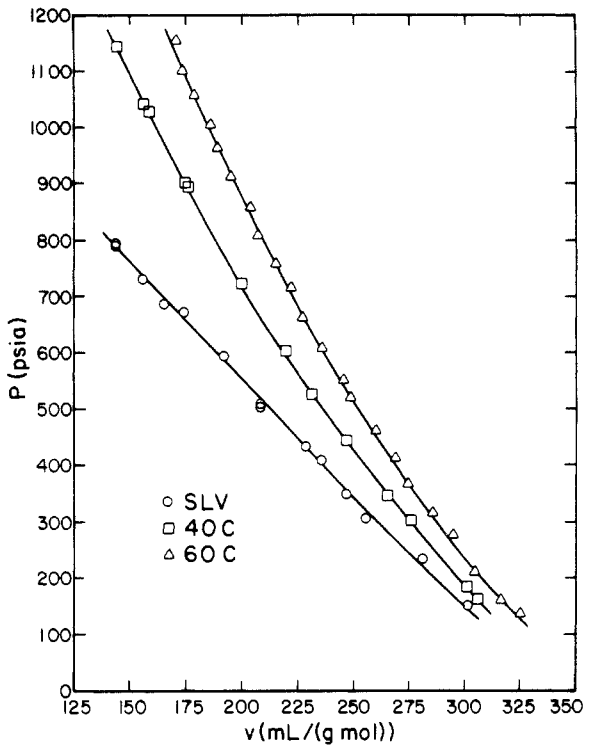

Figure 2. Pressure vs. liquid-phase molar volume for the binary system CO_2 + *n*-nonadecane (14.5 psia = 1 bar).

Tables III and IV are analogous to Tables I and II for the binary system CO_2 + *n*-heneicosane, with Table III being LV raw data at 45 and 65 °C. Figures 3 and 4 graphically illustrate the data in Tables III and IV.

For all of these raw data, it is assumed that the gas phase is pure CO_2. The temperatures should be good to ±0.01 K for the LV equilibria and +0.03 K for the SLV equilibria. All pressures are estimated to be good to ±0.07 bar (1 psia). For the LV studies the liquid-phase mole fractions should be good to ±0.002, and the liquid-phase molar volumes should be good to ±1.2 mL/g-mol. These estimates are based on the average absolute deviations (AAD) of the LV raw data from the smooth curves shown in Figures 1–4; the AAD for the liquid-phase mole fractions is 0.0019, while the AAD for the liquid-phase molar volumes is 1.0 mL/g-mol.

The goodness of the SLV raw data is somewhat less than that of the LV data due to the added difficulty of determining SLV equilibria points in the visual cell. In these studies, the liquid-phase mole fractions should be good to ±0.003 (AAD = 0.0027), and the liquid-phase molar volumes should be good to ±2.5 mL/g-mol (AAD = 2.3 mL/g-mol).

Table III. Pressure, Liquid-Phase Composition, and Molar Volume Raw Data for Liquid-Vapor Isotherms of Carbon Dioxide + *n*-Heneicosane

press., bar	$[CO_2]$, mole fraction	molar vol, mL/(g-mol)
Temperature = 45 °C (318.15 K)		
11.45	0.1402	333.5
22.26	0.2565	295.2
26.86	0.3004	277.9
31.85	0.3451	266.3
36.62	0.3859	249.3
42.40	0.4302	238.1
44.48	0.4472	228.9
51.97	0.4979	215.2
56.61	0.5308	201.3
62.36	0.5629	193.3
65.60	0.5850	183.1
73.68	0.6257	172.2
77.59	0.6496	161.3
Temperature = 65 °C (338.15 K)		
9.31	0.0999	355.3
14.07	0.1460	340.7
19.99	0.2074	318.3
25.76	0.2536	303.7
32.99	0.3142	282.2
36.79	0.3397	273.8
47.32	0.4119	249.1
47.36	0.4106	248.8
57.97	0.4745	227.3
65.27	0.5088	215.4
67.15	0.5256	209.6
77.68	0.5704	193.8
78.20	0.5786	190.8

Table IV. Temperature, Pressure, Liquid-Phase Composition, and Molar Volume Raw Data for the Solid-Liquid-Vapor Locus of Carbon Dioxide + *n*-Heneicosane

temp, K	press., bar	$[CO_2]$, mole fraction	molar vol, mL/(g-mol)
311.24	10.94	0.1468	329.1
310.73	14.76	0.1881	317.7
309.14	22.53	0.2841	282.3
308.07	29.81	0.3543	260.3
306.88	34.76	0.4167	237.1
305.47	43.30	0.4863	216.6
304.42	47.83	0.5376	196.5
303.26	55.48	0.5948	180.9
302.20	62.95	0.6647	154.9
301.89	65.80	0.6798	152.5
301.49	69.39[a]		
301.51	69.34[a]		

[a] Q-point location, L_1 phase dominant.

Raw data for the LLV loci of CO_2 + *n*-nonadecane and CO_2 + *n*-heneicosane are presented in Tables V and VI. Graphs of the L_1 and L_2 composition and molar volume data for these two binary systems are presented in Figures 5–8. Additionally, LLV data were taken for the binary system CO_2 + *n*-eicosane, a system studied previously by Huie et al. (2). Raw data for CO_2 + *n*-eicosane are given in Table VII. The mole fractions reported should be good to ±0.001 while the molar volumes should be good to ±1.0 mL/g-mol. The AAD for both the compositions of L_1 and L_2 is 0.0008, while the AAD's for the molar volumes of L_1 and L_2, respectively, are 0.8 and 0.5 mL/g-mol. As before, the AAD's are based on a comparison of the raw data with the smoothed curves as given in Figures 5–8.

The data of Huie et al. (*2*) agree reasonably well with our data given in Table VII. Absolute deviations in the composition of L_1 are no more than 0.01, while molar volumes agree to

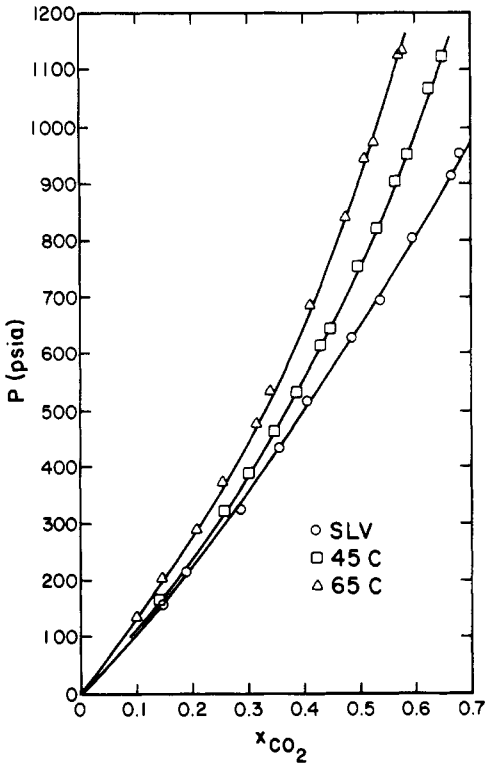

Figure 3. Pressure vs. liquid-phase mole fraction of CO_2 for the binary system CO_2 + *n*-heneicosane (14.5 psia = 1 bar).

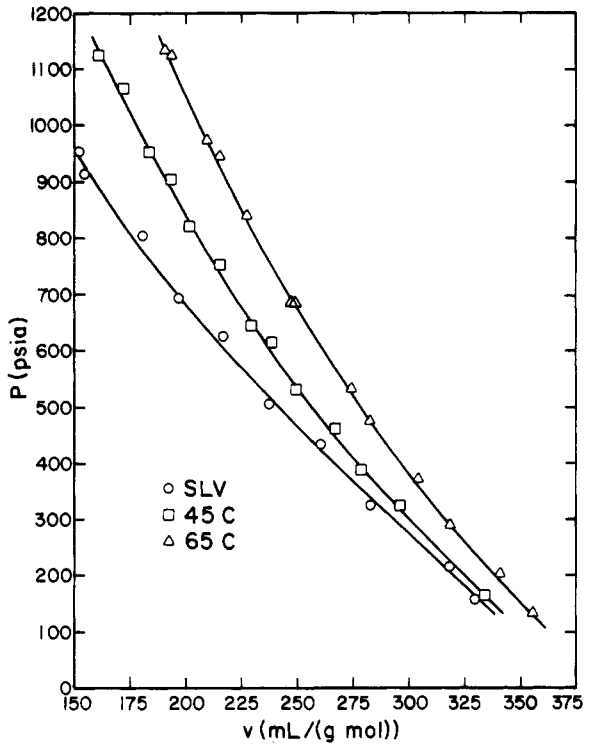

Figure 4. Pressure vs. liquid-phase molar volume for the binary system CO_2 + *n*-heneicosane (14.5 psia = 1 bar).

within ±3%. It should be noted that the purity of the *n*-eicosane used herein is probably superior to that used by Huie et al.; minor discrepancies have been found earlier in the Huie et al. data (*8*).

Remarks

The data in Tables II and IV–VII and ref *2* and *8* demonstrate that the heaviest *n*-paraffin to be LLV immiscible with

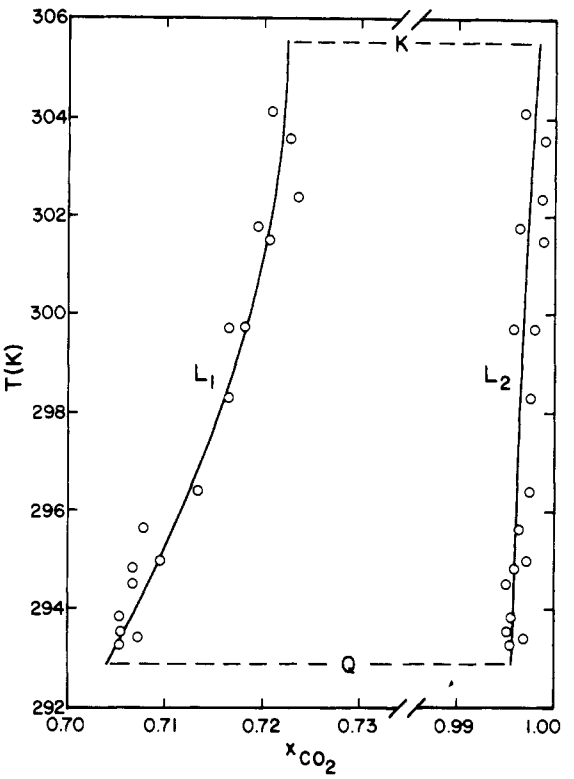

Figure 5. Composition as a function of temperature for the L_1 and L_2 phases for the LLV locus of CO_2 + *n*-nonadecane.

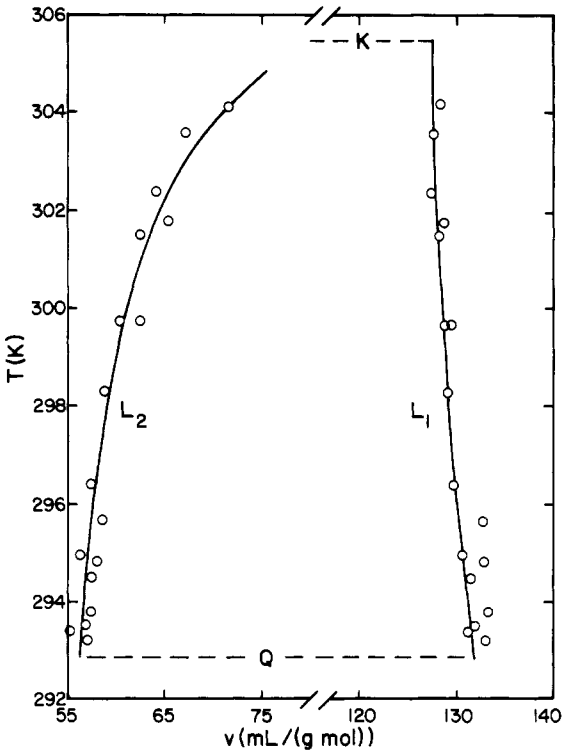

Figure 6. Molar volume as a function of temperature for the L_1 and L_2 phases for the LLV locus of CO_2 + *n*-nonadecane.

CO_2 is that of carbon number 21, *n*-heneicosane. This can be readily seen if one examines the relative positions of the SLV and LLV loci for each binary system, as illustrated in Figure 9. The LLV loci for the binary systems are almost coincident, and the upper critical end points (K points, or L–L=V) are close together, their temperatures decreasing with increasing carbon number. The location of the Q points is more sensitive to

Table V. Raw Data for the LLV Locus of the Binary System CO_2 + *n*-Nonadecane

		L_1 phase		L_2 phase	
temp, K	press., bar	$[CO_2]$, mole fraction	molar vol, mL/(g-mol)	$[CO_2]$, mole fraction	molar vol, mL/(g-mol)
292.88	56.68[a]				
293.23	57.14	0.7052	133.0	0.9955	57.1
293.40	57.41	0.7071	131.1	0.9969	55.3
293.54	57.47	0.7052	131.8	0.9951	57.0
293.81	57.96	0.7052	133.1	0.9957	57.5
294.49	58.80	0.7068	131.5	0.9951	57.7
294.81	59.31	0.7068	132.8	0.9959	58.1
294.95	59.53	0.7095	130.6	0.9971	56.3
295.65	60.46	0.7078	132.7	0.9963	58.6
296.40	61.54	0.7133	129.7	0.9973	57.2
298.32	64.33	0.7165	129.0	0.9975	58.8
299.77	66.56	0.7181	128.7	0.9979	60.4
299.79	66.19	0.7165	129.4	0.9958	62.4
301.52	69.13	0.7206	128.1	0.9988	62.4
301.79	69.43	0.7195	128.6	0.9964	65.3
302.39	70.53	0.7237	127.3	0.9988	64.1
303.60	72.58	0.7228	127.6	0.9990	67.0
304.17	73.21	0.7209	128.6	0.9969	71.5
305.47	75.81[b]				
305.51	75.75[b]				

[a] Q-point location, L_2 phase dominant. [b] K-point location, L_1 phase dominant.

Table VI. Raw Data for the LLV Locus of the Binary System CO_2 + *n*-Heneicosane

		L_1 phase		L_2 phase	
temp, K	press., bar	$[CO_2]$, mole fraction	molar vol, mL/(g-mol)	$[CO_2]$, mole fraction	molar vol, mL/(g-mol)
301.47	69.22[b]				
301.51	69.34[a]				
301.78	69.75	0.7087	142.6	0.9976	65.7
301.89	69.93	0.7077	143.7	0.9993	64.4
302.17	70.41	0.7096	142.4	0.9977	66.7
302.33	70.66	0.7084	143.1	0.9995	65.3
302.63	71.13	0.7092	142.8	0.9978	67.6
302.81	71.44	0.7092	142.9	0.9995	66.5
303.08	71.84	0.7091	142.9	0.9979	68.8
303.37	72.33	0.7095	142.9	0.9996	68.2
303.61	72.75	0.7090	143.3	0.9997	68.9
303.87	73.19	0.7086	143.4	0.9983	72.1
304.97	74.99[c]				
304.98	75.07[d]				

[a] Q-point location, L_1 phase dominant. [b] Q-point location, L_2 phase dominant. [c] K-point location, L_1 phase dominant. [d] K-point location, L_2 phase dominant.

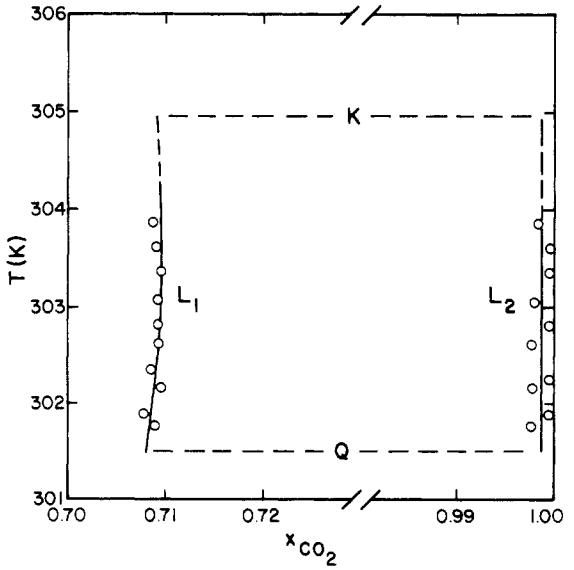

Figure 7. Composition as a function of temperature for the L_1 and L_2 phases for the LLV locus of CO_2 + *n*-heneicosane.

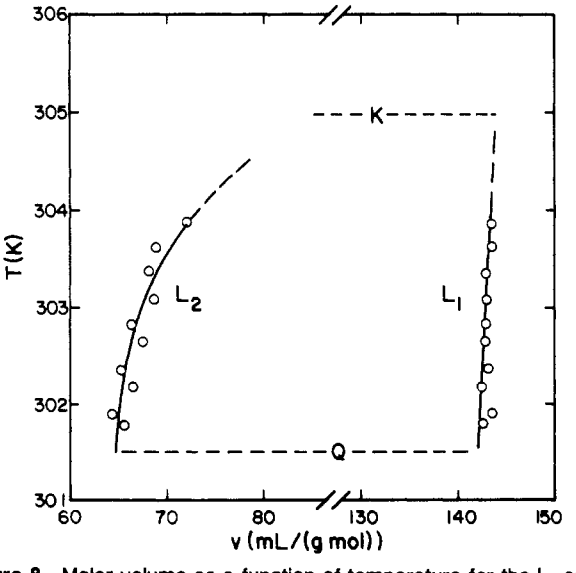

Figure 8. Molar volume as a function of temperature for the L_1 and L_2 phases for the LLV locus of CO_2 + *n*-heneicosane.

carbon number. Each Q point is the junction of the SLV locus and the LLV locus, and the position of the SLV locus is governed to a large degree by the location of the triple point of the *n*-paraffin which is its lower terminus. As the carbon number increases, so does the triple point temperature. For carbon number 22, *n*-docosane, the SLV locus passes *above* the re-

Table VII. Raw Data for the LLV Locus of the Binary System CO_2 + *n*-Eicosane

		L_1 phase		L_2 phase	
temp, K	press., bar	$[CO_2]$, mole fraction	molar vol, mL/(g-mol)	$[CO_2]$, mole fraction	molar vol, mL/(g-mol)
300.33	67.34[a]				
300.39	67.51	0.7162	134.9	0.9986	61.4
300.53	67.66	0.7168	134.8	0.9985	61.6
300.63	67.71	0.7150	136.1	0.9986	61.5
300.73	67.94	0.7160	135.1	0.9986	61.9
301.12	68.42	0.7166	135.4	0.9987	62.3
301.17	68.73	0.7162	135.3	0.9985	62.6
301.42	68.86	0.7169	135.3	0.9987	62.7
301.52	69.22	0.7159	135.5	0.9987	63.0
301.62	69.42	0.7148	133.7	0.9973	65.0
301.89	69.77	0.7153	135.8	0.9990	63.6
302.11	70.19	0.7151	136.0	0.9990	64.1
302.13	69.89	0.7152	136.3	0.9988	64.0
302.46	70.71	0.7147	136.4	0.9997	64.7
302.78	71.20	0.7162	135.8	0.9998	65.5
303.06	71.66	0.7152	136.2	0.9998	66.3
303.28	71.84	0.7164	131.7	0.9998	66.7
303.36	72.13	0.7147	136.7	0.9976	68.1
303.50	72.45	0.7123	135.4	0.9977	69.7
304.10	73.48	0.7141	134.8	0.9981	72.4
304.60	74.28	0.7161	133.9	0.9985	74.9
305.24	75.40[b]				

[a] Q-point location. [b] K-point location.

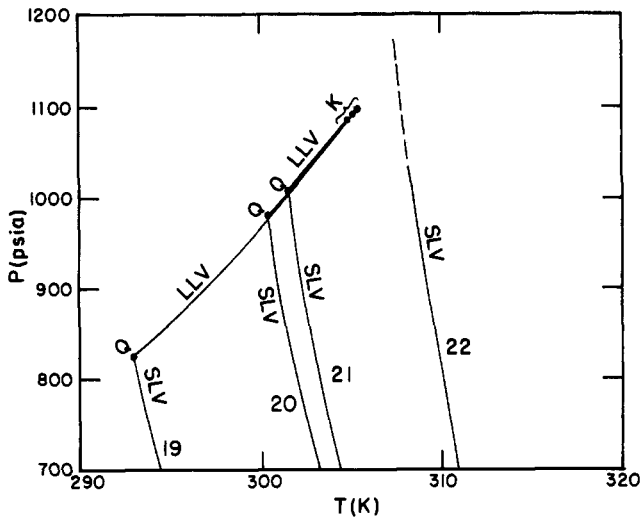

Figure 9. Pressure–temperature plot of the SLV and LLV loci for CO_2 + *n*-paraffin binary systems with carbon numbers 19–22.

gion where the K-point terminus of the LLV locus is usually found, and consequently no LLV locus occurs.

Appendix

Mass Balances for the LLV Problem. It is assumed throughout that the vapor phase is pure CO_2 of known compressibility factor z and volume V_v. Thus, the mass balance will apply only to the two liquid phases L_1 and L_2. For a binary system, the LLV locus has one degree of freedom. If one fixes the temperature T along the locus, one has an invariant state. The procedure for experimentally determining the compositions of L_1 and L_2 of the particular state of interest is to perform two experiments at a given fixed temperature, one with $V_{L_1} \gg V_{L_2}$ ("L_1-dominant experiment") and the other with $V_{L_2} \gg V_{L_1}$ ("L_2-dominant experiment"). Denote the information for these two experiments by superscripts 1 and 2, respectively.

For each of the experiments we know the following: N_{TOT} = total number of moles in $L_1 + L_2$; x_1 = overall CO_2 mole fraction in $L_1 + L_2$; V_{L_1} = volume of L_1 phase; V_{L_2} = volume of L_2 phase. Let u_1 be the mole fraction of CO_2 in L_1, and w_1 be the mole fraction of CO_2 in L_2. u_1 and w_1 do not vary between the two experiments. Mass balances in the form of lever principles give

$$\frac{N_{L_1}^{(1)}}{N_{TOT}^{(1)}} = \frac{w_1 - x_1^{(1)}}{w_1 - u_1}$$

$$\frac{N_{L_1}^{(2)}}{N_{TOT}^{(2)}} = \frac{w_1 - x_1^{(2)}}{w_1 - u_1}$$

Also, one can define the ratios

$$N_{L_1}^{(2)}/N_{L_1}^{(1)} = V_{L_1}^{(2)}/V_{L_1}^{(1)} = \alpha$$

$$N_{L_2}^{(2)}/N_{L_2}^{(1)} = V_{L_2}^{(2)}/V_{L_2}^{(1)} = \beta$$

where α and β are known from the experiments. For the experiments as described, $\alpha \ll 1$ and $\beta \gg 1$. Combining these four equations leads to the compositions of L_1 and L_2:

$$u_1 = \frac{x_1^{(1)} - (x_1^{(2)} N_{TOT}^{(2)}/\beta N_{TOT}^{(1)})}{1 - (N_{TOT}^{(2)}/\beta N_{TOT}^{(1)})}$$

$$w_1 = \frac{x_1^{(2)} - (x_1^{(1)} \alpha N_{TOT}^{(1)}/N_{TOT}^{(2)})}{1 - (\alpha N_{TOT}^{(1)}/N_{TOT}^{(2)})}$$

In turn, it follows that

$$N_{L_1}^{(1)} = N_{TOT}^{(1)}\left(\frac{w_1 - x_1^{(1)}}{w_1 - u_1}\right)$$

$$N_{L_2}^{(2)} = N_{TOT}^{(2)}\left(\frac{x_1^{(2)} - u_1}{w_1 - u_1}\right)$$

which yield the L_1 and L_2 molar volumes as

$$V_{L_1} = V_{L_1}^{(1)}/N_{L_1}^{(1)}$$

$$V_{L_2} = V_{L_2}^{(2)}/N_{L_2}^{(2)}$$

Registry No. CO_2, 124-38-9; nonadecane, 629-92-5; heneicosane, 629-94-7; eicosane, 112-95-8.

Literature Cited

(1) Im, V. K.; Kurata, F. J. Chem. Eng. Data 1971, 16, 412-5.
(2) Huie, N. C.; Luks, K. D., Kohn, J. P. J. Chem. Eng. Data 1973, 18, 311-3.
(3) Schneider, G.; Alwani, Z.; Heim, W.; Horvath, E.; Franck, E. Chem-Ing.-Tech. 1967, 39, 649-56.
(4) Schneider, G. Chem. Eng. Prog. Symp. Ser. 1968, 64, 9-15.
(5) Schneider, G. Adv. Chem. Phys. 1970, 17, 1-42.
(6) Hottovy, J. D.; Luks, K. D.; Kohn, J. P. J. Chem. Eng. Data 1981, 26, 256-8.
(7) Kulkarni, A. A.; Zarah, B. Y.; Luks, K. D.; Kohn, J. P. J. Chem. Eng. Data 1974, 19, 92-94.
(8) Fall, D. J.; Luks, K. D. J. Chem. Eng. Data 1984, 29, 413.
(9) Varagftik, N. B. "Tables on the Thermophysical Properties of liquids and Gases", 2nd ed.; Wiley: New York, 1975, pp 167-8.

Received for review April 30, 1984. Accepted August 2, 1984. Support for this research was provided by the National Science Foundation (grant no. CPE-8100450). The apparatus used is part of the *PVTx* Laboratory at The University of Tulsa and was purchased with funds provided by several industries, The University of Tulsa, and a National Science Foundation specialized equipment grant (no. CPE-8014650).

Solubilities of Toluene and *n*-Octane in Aqueous Protosurfactant and Surfactant Solutions

Patience C. Ho

Chemistry Division, Oak Ridge National Laboratory, Oak Ridge, Tennessee 37831

The solubilities of toluene and *n*-octane in aqueous protosurfactant and surfactant solutions were determined at 25 °C. The protosurfactants studied are sodium salts of cyclohexanecarboxylic acid, 2,5-diisopropylbenzenesulfonic acid, and 3,5-diisopropylsalicylic acid. Each of them has six alkyl carbons (S_{AC} = 6) and does not form micelles in water. The two micelle-forming surfactants used are sodium *n*-hexanoate with six alkyl carbons (S_{AC} = 6) and sodium *n*-octanoate with eight alkyl carbons (S_{AC} = 8). In three-component systems of toluene or *n*-octane with water and organic salt (either protosurfactant or surfactant), the solubility of the hydrocarbon in the aqueous phase increases as the number of alkyl carbons of the organic salt and as the aqueous concentration of the organic salt increases. However, in this study we found that sodium 3,5-diisopropylsalicylate causes much more pronounced increases in hydrocarbon solubility than these two surfactants. Sodium 2,5-diisopropylbenzenesulfonate, although not as effective in solubilization as the salicylate, has much stronger hydrotropic properties for hydrocarbons than either of these two surfactants. Sodium cyclohexanoate, with a compact arrangement of the six alkyl carbons, shows a higher hydrotropic effect than sodium *n*-hexanoate.

Introduction

In two previous papers (*1*, *2*) we have presented the hydrotropic effect of low-equivalent-weight organic salts, "protosurfactants". In this paper we compare the hydrotropic effect of three protosurfactants with two low-equivalent-weight surfactants.

The three protosurfactants are sodium 2,5-diisopropylbenzenesulfonate, sodium 3,5-diisopropylsalicylate, each of which has six alkyl carbons on the benzene ring, and sodium cyclohexanoate, which also has six alkyl carbons. The two alkyl-substituted aromatic sulfonate and hydroxybenzoate may form small aggregates (*3*), but there is no evidence of micellar formation. Sodium cyclohexanoate, which has a compact arrangement of the six alkyl carbons, also does not form micelles (*4*). The two surfactants chosen to study are sodium *n*-hexanoate with six alkyl carbons and sodium *n*-octanoate with eight alkyl carbons. Although there appears to be no definite cmc (critical micellar concentration) value for sodium *n*-hexanoate, it is reported to form small aggregates at lower concentration (*5-7*), which increase to the micellar range as the concentration increases (above 1.2 M) (*6*), and become quite large at high concentration (*6*, *7*). Sodium *n*-octanoate forms moderate-size micelles at lower concentration (the cmc of octanoate at 25 °C is reported to be 0.39 mol/(kg of H_2O)) (*8*) and the micelle number is said to increase approximately linearly with concentration relative to the cmc (*9*).

The primary goal of this study is to compare the hydrotropic effect (or solubilization of hydrocarbons in water) of these organic salts (protosurfactant and surfactant) with an equivalent number of alkyl carbons but different structural arrangement. The solubilities of toluene and *n*-octane in aqueous solutions of either sodium *n*-hexanoate or sodium *n*-octanoate were found to be much lower than in aqueous solutions of sodium 2,5-diisopropylbenzenesulfonate and sodium 3,5-diisopropylsalicylate at corresponding aqueous concentrations.

Experimental Section

Materials. The source of toluene, sodium 2,5-diisopropylbenzenesulfonate, and sodium 3,5-diisopropylsalicylate used in this study can be found in ref *1* and *2*. Sodium *n*-hexanoate (Tokyo Kasei/TCI), sodium *n*-octanoate (BDH Lab), and *n*-octane (Aldrich) were used as received without further purification. Cyclohexanecarboxylic acid (Fluka AG) was converted to the sodium salt by titration to pH 7 with 10% NaOH. After the titration the solutions were filtered and washed several times with $CHCl_3$ to remove excess acid and the salt was crystallized after volume reduction. The crude product was recrystallized 2 more times from water. Analysis of this salt was done by Galbraith Laboratories, Inc., Knoxville, TN, and the results are as follows. Anal. Calcd: C, 55.97; H, 7.39. Found: C, 55.94; H, 7.41.

The aqueous organic salt solutions were prepared with distilled water, and concentrations are expressed in terms of molality, *m* (mol/(kg of H_2O)).

Methods. The hydrocarbon-saturated aqueous solutions were prepared as follows: In a 6-mL Hypo-vials (Pierce), 1 mL of hydrocarbon was added to 2 mL of distilled water or aqueous salt solutions; then the vials were sealed with neoprene septa (Pierce) and aluminum seals. The vials were shaken vigorously for ca. 10 min and put upside down into a test tube which was set inside a 25 ± 1 °C water bath for equilibration for at least 4 days. In between, the vials were shaken gently several times in order to get rid of any tiny hydrocarbon drops from the

0021-9568/85/1730-0088$01.50/0